

Automatic Optical Detection of Indentation into Polymers for Inner Stress Analysis

Lukáš Bureš, Marek Hruz, Luděk Müller

European Centre of Excellence
NTIS - New Technologies for the Information Society
Faculty of Applied Sciences, University of West Bohemia
Univerzitní 22, 306 14 Plzeň, Czech Republic
lbures@ntis.zcu.cz; mhruz@ntis.zcu.cz; muller@ntis.zcu.cz

David Mañas, Miroslav Mañas

Tomas Bata University in Zlín
nám. T. G. Masaryka 5555, 760 01 Zlín, Czech Republic
dmanas@ft.utb.cz; manas@ft.utb.cz

Abstract – In this paper we present a method for automatic detection of Vickers indentation into polymers using computer vision techniques. Since the polymers relax after the indentation process we track the changes of the indentation and correlate the results with the inner stress of the polymer. The stress was applied by bending. Our results show that change in the shape of the indentation is correlated with the bending level. This knowledge can be utilized in applications of quality measurement.

Keywords: PMMA, Inner stress, Vickers micro-hardness test, Relaxation, Image processing.

1. Introduction

With the development of production methods new materials were introduced. Quality of these materials is a key issue. In metallurgy micro-hardness testing is often used to measure the quality of materials. In recent years these tests were extended to other materials. In the case of polymers the indentation is not static but as the material relaxes the indentation becomes smaller. It can be hypothesized that the process of the relaxation indicates the quality of the material. In this paper we present a computer vision method for detecting the indentation in images and utilize the detection to verify our hypothesis. The test object is a PMMA. A PMMA is routinely produced by emulsion polymerization, solution polymerization, and bulk polymerization. We examine test objects which are defined by stress brought into the state of internal stress. This is achieved by precisely defined test preparatives (see Fig. 1), with different radius, which set the state of stress into the test specimen. With a larger radius of the curvature, the degree of stress in the specimen becomes greater. For the purposes of this paper we use the difference between the tip and the bottom of the bended test object as an indicator of applied stress.



Fig. 1. The preparative for applying the stress to the test object.

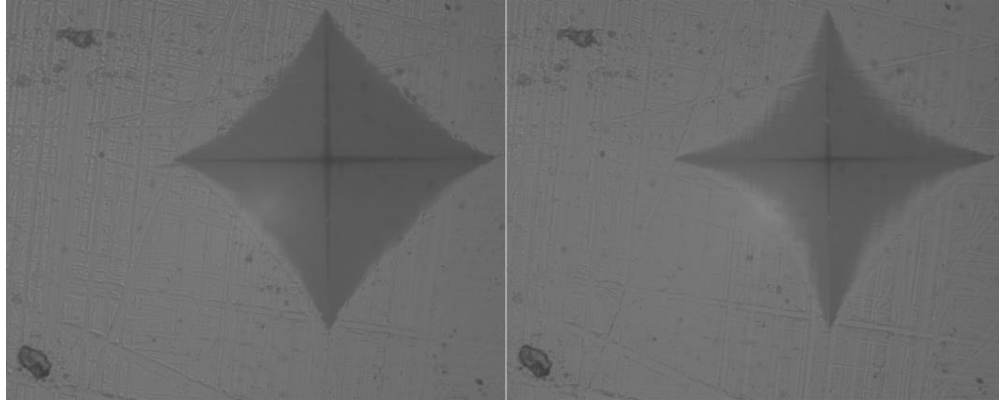


Fig. 2. In the left image an indentation immediately after removing the indenter is shown. In the right image an indentation after relaxation is shown.

We do tests of micro-hardness according to Vickers. This test is prescribed by European standard ČSN EN ISO 6507-1. Example of a resulting indentation can be seen in Fig. 2.

Our hypothesis is that, if the internal stress of the PMMA specimen is greater, then the indentation after relaxation is smaller. For verification it is necessary to accurately detect the indentation and compare the area of indentation before and after relaxation.

2. Image Segmentation

The goal of image segmentation is to obtain the most accurate position of the corner points and the centroid of the indentation. Usually some kind of noise is present in the image data. In our case there is a row noise that we are able to suppress / eliminate by appropriate methods.

Next, we use a combination of Otsu's adaptive threshold method (Otsu, 1979) and variance image calculated using integral image. We obtain a binary image in which the value 'one' represents the interior of the indentation. These values are summed row-wise and the maximum is found over these sums. The row with the maximum value determines the y-value of the right and the left corner point and vice versa for column. From these corner points the mean value is calculated for estimating the position of the centre point of the indentation. The centre point and corner points are marked by a green star and green circles in Fig. 3 on the left side.

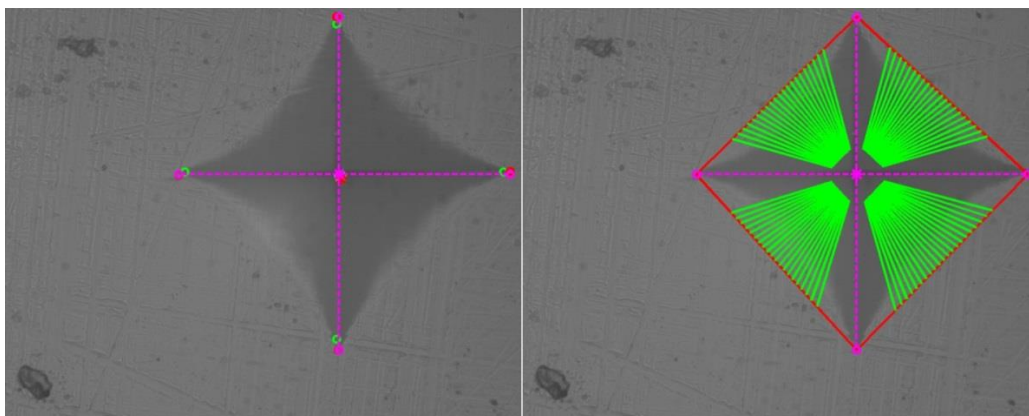


Fig. 3. Left image shows the detected and enhanced centre and corner points. Right image shows cone of lines pointing from the centre point of indentation to the straight line which connect the corner points.

The obtained corner points do not exactly match the real corners of the indentation. It is necessary to improve their position. Improved positions of corner points V_R and the centre point S_R are shown in Fig. 3 on the left side. They are marked by red circles and a star.

In the middle of the indentation there is a black cross. It is used to adjust the final position of the centre point S^* . The cross together with the centre point S_R is used in an iterative algorithm that finds the centre point S^* . The sub-image around S_R and the same method, as described in the second paragraph of this section are used. The algorithm for searching S^* is usually finished after the third iteration. It will stop if the centre points of two consecutive iterations are identical or if it reached the maximum number of iterations. The calculated centre point S^* of indentation is shown in Fig. 3 on the left side marked with purple star.

Due to these changes of the centre point S^* it is necessary to adjust the positions of the corner points V_R to better fit the geometry of the indentation. We use the centre point S^* and corner points V_R for calculating the resulting corner points V^* . For these corner points V^* , one coordinate value is always fixed and the second is replaced by the appropriate coordinate value of the centre point S^* . Positions of corner points V^* are shown in Fig. 3 with purple circles. They are connected with the centre point S^* with purple dashed lines.

3. Edges Localization

It is necessary to determine the indentation's edge as accurately as possible. Indentation is divided according to the major axes into the four quadrants that are ideally symmetrical. The indentation edge is evaluated in every quadrant independently. In each quadrant 62 lines are constructed and 21 of them can be seen in Fig. 3 on the right side. The lines are led away from the centre starting about 10% of length of the lines away from the centre and are led to the junction of the corner points (red lines). The lines are designed in such a fashion that there is 15° of blank space on each side.

Each of the lines consists of equidistant points. For every point we compute a grayscale value as a mean value of pixels in a surrounding area. The grayscale values for the upper-left quadrant of the indentation in Fig. 3 can be seen in Fig. 4 on the left side. The first derivate of the values in the line segment is calculated. After that, a local variance over a window is calculated and it is plotted in Fig. 4 on the right side. We omit windows that contain any negative values of the derivate to avoid the detection of inappropriate edge transitions. The edge position of the indentation for a given line is determined by the position of the maximum value of the variance. The final positions of the edges can be seen in Fig. 5 which are shown as purple crosses on the edges of the indentation.

The shape of the indentation edge is considered to be a second order polynomial. Hence we robustly interpolate the detected edges' points using parabola formulae and weights. Corners of the indentation were assigned a large weight so that the parabola always goes through them. All the other edge points were assigned a smaller weight. To obtain a better result of the interpolation we rotate the edge points so that the diagonal line passing the current quadrant becomes the y-axis. After the interpolation is computed an inverse transformation of rotation is applied to the resulting parabola. This way we obtain a better interpolation of the data which corresponds with the physical model of the indenter. Resulting parabolas can be seen in Fig. 5 and are shown in cyan colour. The whole process of the detection lasts ~2 seconds on a standard PC.

4. Experiments

The aim of our experiment is to analyze the relaxation process that is taking place in the polymer after the indentation. The analysis is preformed on visual data. We want to find out whether the visual cues are dependent on the inner stress of the polymer. This can lead to a novel approach for measuring the quality of the polymer. For this task we need to obtain information about the change in the area of the indentation.

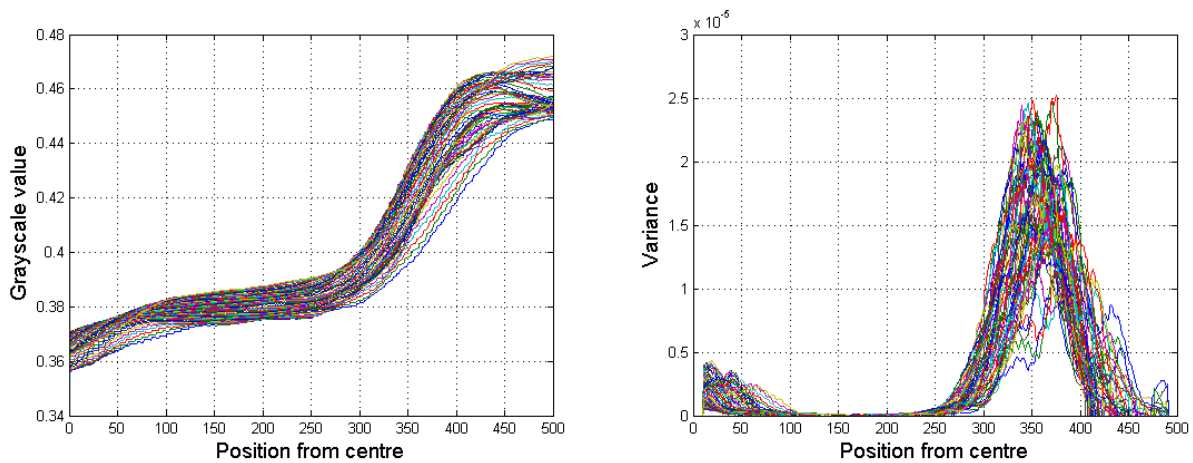


Fig. 4. Left image shows mean grayscale value of top left quadrant of Fig. 2. Right image shows variance of derivate of data in left image.

The data set used in our experiment consisted of 5 time series depicting the relaxation of the polymer. Each of the series contained 40 time frames for 11 different bend values 1.4, 1.2, 1.0, 0.8, 0.7, 0.6, 0.5, 0.4, 0.3, 0.2, and 0.0 cm. Each time series was measured in time spaced at 12 second interval. Each time frame represents one image of one indentation taken at this time frame. For the next analysis we used only the first and the last frame (i.e. two images) of each time series, so the time between the first and the last time frame of each time series is 10 minutes. In this way we obtained $5 \times 11 = 55$ image pairs. Because some of the images contained defects in the material in the place of indentation we had to exclude them from the next experiments. After this exclusion, the data set was reduced to 41 image pairs. The summary can be seen in Table 1.

Table 1. The values of the bend and corresponding number of image pairs and RQIAs. The rows corresponding to the bend values that had zero image pairs are omitted.

Bend [cm]	Number of image pairs	RQIA
0.2	4	4
0.3	5	5
0.4	5	5
0.5	5	5
0.6	4	4
0.7	5	5
0.8	5	5
1.2	4	4
1.4	4	4

Furthermore, each (undamaged) image was split into 4 subimages, i.e. to 4 quadrants depicted in Fig. 5., thus for each image pair we acquired 4 corresponding subimage pairs - each of these pairs contained 2 images: a first time frame quadrant subimage (FQS) and a last time frame quadrant subimage (LQS).

Because we assumed that the rate of the relaxation of the polymer in the place of the indentation is higher for higher values of bend than for its smaller values and vice versa, we tried to use this knowledge for finding a suitable feature set for a bend classifier. We proceeded as follows: For each FQS we

calculated its area (let us denote it as FQSA) and similarly for each LQS its area LQSA. Then for each subimage pair we calculated the ratio of LQSA to FQSA:

$$RQSA = \frac{LQSA}{FQSA} \quad (1)$$

Finally, for each image pair I the ratio RQIA was estimated as a median of all 4 RQSA values of the image pair I . With this procedure we obtained 41 RQIA values (each RQIA for one of the 41 image pairs see Table 1.). These 41 RQIA values created our feature set which has been further analysed.

The aim of our work was primarily to prove that the image pairs contain sufficient information necessary to distinguish between the levels of the bend. Our idea was as follows: When (in some appropriate manner) we will be able to find such a feature set (e.g. RQSA) whose features are correlated with the corresponding bend values then the images probably contain sufficient information necessary for a proper operation of the bend classifier. To verify the assumption that the image processing approach described above is applicable, we calculated the correlation between the RQIA values and their corresponding bend values. Because we can assume that neither RQIA nor the bend values have a normal distribution, in addition to Pearson's correlation coefficient (Pearson K. (1896, 1900, 1920)) Rho_p , we also computed Kendall's (Kendall M. G. (1938, 1948)) and Spearman's (Spearman C. E. (1904a, 1904b, 1910)) correlation coefficients Rho_K and Rho_S , which are based on order statistics. Finally, a statistical test that the correlation is significantly different from zero was performed for all these three correlation coefficients. The results of the test were:

Pearson's correlation coefficient $Rho_p = -0.3235$ ($p < 0,04$)
 Kendall's correlation coefficient $Rho_K = -0.1943$ ($p < 0,09$)
 Spearman's correlation coefficient $Rho_S = -0.264$ ($p < 0,10$)

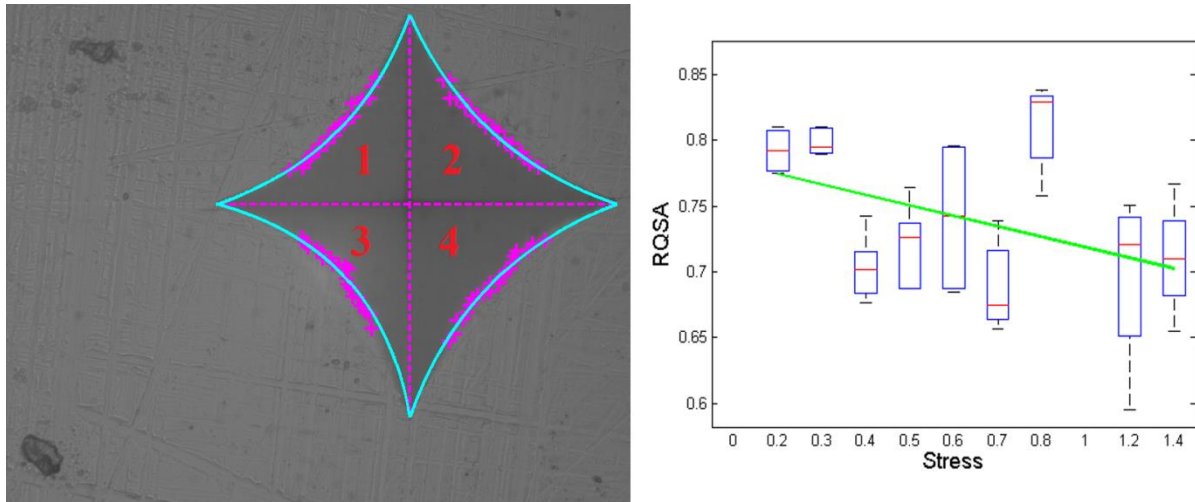


Fig. 5. Left: Interpolated points using a second order polynomial. The numbers refer to quadrants. Right: Dependence of the RQSA on the applied stress. The green line is a linear representation of the dependence. On each box, the central mark is the median, the edges of the box are the 25th and 75th percentiles, and the whiskers extend to the most extreme data points.

Although the Kendall's and Spearman's correlation coefficients are nonzero with p -value greater than 0.05 their p -value is still below 0.1 which indicates that both the processed images and the RQIA features may contain some amount of useful information about the corresponding level of the bend. Furthermore, all three correlation coefficients have a negative value which corresponds to the fact that the RQIA value

is decreasing with increasing level of bend. In other words, the higher the value of the bend is the smaller the final area of indentation is. Fig. 5. illustrates this dependence.

We assume that with more amounts of data we could achieve even more statistically significant results. Therefore, in future work we plan to deal with a larger data set as well as to try to find and investigate even more sophisticated (and more informative) features.

5. Conclusion

In this paper we presented a method for the detection of indentation into a PMMA polymer. The result of the detection is a parametric model of the indentation. Features in the form of pixel area in each quadrant are used to compute a correlation with the level of bend applied to the test object. The results show a tendency in the relaxation of the material with different inner stress. Materials with greater stress relax more rapidly. This means that the final indentation has a smaller area. Such tests can be performed to analyze the inner stress of a polymer to measure the quality of the material. Polymers with higher inner stress tend to break more. In the future we would like to automate the micro-hardness measurement testing. For this purpose we will need labelled data. With more data we will obtain better results. Lastly we want to develop improved and enhanced methods. Our final goal is to classify the level of inner stress in the polymer.

Acknowledgements

This work was supported by the European Regional Development Fund (ERDF), project “NTIS - New Technologies for Information Society”, European Centre of Excellence, CZ.1.05/1.1.00/02.0090.

Access to computing and storage facilities owned by parties and projects contributing to the National Grid Infrastructure MetaCentrum, provided under the programme "Projects of Large Infrastructure for Research, Development, and Innovations" (LM2010005), is greatly appreciated.

References

- Kendall M. G. (1938). “A New Measure of Rank Correlation.” *Biometrika* 30: 81-89
- Kendall M. G. (1948). “Rank correlation methods.” 4th ed. Griffin, London.
- Otsu N. (1979). “A threshold selection method from gray-level histograms.” *IEEE Trans. On Systems, Man and Cybernetics* 9 (1): 62–66.
- Pearson K. (1896). “Mathematical contribution to the theory of evolution. III. Regression, heredity, and panmixia.” *Philosophical Transaction of the Royal Society Ser. A* 187: 253-318
- Pearson K. (1900). “Mathematical contribution to the theory of evolution. VII. On the correlation of characters not quantitatively measurable.” *Philosophical Transaction of the Royal Society Ser. A* 195: 1-47
- Pearson K. (1920). “Notes on the history of correlation.” *Biometrika* 13: 25-45
- Spearman C. E. (1904a). “The proof and measurement of association between two things.” *American Journal of Psychology* 15: 72-101
- Spearman C. E. (1904b). “General intelligence, objectively determined and measured.” *American Journal of Psychology* 15: 201-293
- Spearman C. E. (1910). “Correlation calculated from faulty data.” *British Journal of Psychology* 3: 271-295